Specialization project
TTK4551

Project thesis

Virtual Synchronous Machines in hybrid ship power systems

Edvard Grimsmo Hofstad

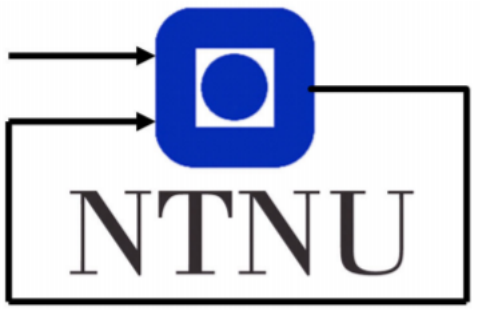

Department of Engineering Cybernetics

June 10, 2019

Supervisor: Jon Are Suul

Preface

This is the report for the subject TTK4551, Specialization Project for Engineering Cybernetics, a *7.5 studypoints* subject for two-year master students. This thesis is written by Edvard Grimsmo Hofstad with Jon Are Suul as supervisor. I want to thank my supervisor, Jon Are, for contributing to the problem description and the guidence he has given me.

Abstract

Energy storage systems are increasingly used in marine power systems in order to reduce fuel consumption. For power distribution on marine vessels, an emerging control structure for inverters called Virtual synchronous machines (VSM) is an alternative approach for simplifying the transition between operations of a hybrid power grid. One of the main objectives for VSM based control is to introduce inertia to an as a traditional synchronous (SM) would contribute to a power grid. This solves the problem with having no swing mass, and deciding how the reference values for frequency and voltage of the system should be controlled. This can be solved by introducing mathematical models of a SM in the control structure of the inverter and from this emulate inertia.

The main focus area for this report are marine power systems. An introduction to the concept of VSM have been formulated, and a implementation have been simulated and tested. The simulation has had two main focuses. Firstly, the VSM should function be able to deliver power to a load in both parallel with strong grid and a SM. The amount of delivered power should be able to change by altering the reference value. Second, the VSM should be able to maintain the grid voltage and frequency when the SM trips. This should be a seamless process, without changing any parameters or control structures. For testing this, a simulation of a marine power system with a VSM have been conducted with various cases relevant for a simplified ship power system. The cases include load change, tripping a islanded connection and tripping the SM leaving the VSM to independently delivering power to the grid.

The results show some of the benefits of implementing a VSM. This includes giving the possibility to emulate inertia to a system that have low or no swing mass at all. This is a method for making a hybrid power solution with renewable energy sources along with the conventional diesel engines, able to reliable and efficient switch between operation without having the need of changing control structure and parameters. It also shows that the system can be maintained by the VSM for different scenarios.

Contents

List of Figures

List of Tables

1 Introduction

1.1 Problem formulation

This project should study the general capabilities of a VSM-controlled power converter, giving an introduction of how such a system can be built. Different methods and different approaches should be evaluated. In addition to this, investigate methods for evaluating how a battery system with VSM-based control can influence the stability and transient response of ship power system in various operating conditions relevant for the function of a VSM.

1.2 Motivation

Energy storage systems are in an increasing rate used in marine power systems. This introduces the possibility of allowing zero emission operation for hybrid power systems. If battery energy storage is utilized in a ship power system with AC-distribution, the most common method for power conversion is three-phase voltage source converters. The most common method for controlling these are implementing a phase locked loop (PLL). This allows the controllers to synchronize the voltage at the AC-bus, usually controlled by the synchronous machines (SM). However, hybrid power systems should be able to operate with only inverters maintaining the grid. Utilizing zero emission operation implies that the SMs in the system are not active, meaning that the swing mass is not present. This will require the inverters to control the voltage and frequency at the AC-bus. There are different ways of doing solving this problem. Using the concept of VSM, the electronic converters can operate independently of the SM, and is able to manage the power grid on its own by using a power source.

1.3 Related work

VSM based control for inverters is a popular research topic worked on continuously. NTNU have researchers working on this subject, and have published results and developed some solutions relevant for this thesis. There are many related articles related to this topic, with various approaches. The project model is built from scratch, but (1) have been used as a inspirational source. The article (2) gives a good introduction of the different ways of implementing and modeling VSM based power control, as well as give an overview of the advantages and disadvantages of the different typologies.

1.4 Approach

The main objective for this thesis is giving an overview of the concept and tests the general capabilities for this type of VSM implementation with different operating scenarios. This includes tripping the Synchronous generator feeding power to the gird parallel to the inverter, load changes and load sharing for the energy sources in the grid using the set point for the VSM. A study of VSM have been conducted and simulated. The theory part should be a literature study, presenting the basic principles of a VSM based control structure. The simulation should be a relevant model of a marine power system, as well should the operating conditions reflect the different scenarios a marine power grid can endure.

2 Theory

This chapter contains a introduction to marine power systems and some of the theory behind the concept of virtual synchronous machines. It introduces the various components of the VSM control structure, and presents some system equations. In the next chapter the implementation will be presented along with block charts.

2.1 Marine power systems

The use of power electronics in marine propulsion systems became around 1980 a common method for improving fuel efficiency, and is at an increasing rate becoming more used. Diesel electric propulsion is commonly used as the main energy source, and alternative sources like batteries are becoming more popular as this solution reduce fuel consumption. As the usage of power electronics increases, hybrid power systems solutions become more common, and the trend could point towards all electric solutions for marine power systems in the not so distant future.(3)

The main difference between land-based power systems and marine propulsion power systems is that the power is generated close to the consumers and a transmission line for power transfer in the same manner as land-based systems is not needed. Because of the voltage level being relatively low, and the installed power high, this leads to special engineering challenges for these systems. The control system for land based operations is spread out and divided in to parts for each area, but for a ship power system the control system will give the possibility to have a much tighter implementation. (4)

Availability for the power system on a ship is important. This is why the electrical network is engineered to be redundant in order to ensure a reliable power system. This can be seen in figure 1. The main switch boards are usually divided into two, three or four sections, obtaining the required redundancy for the power system. Figure 1 has in addition to combustion generators, two batteries feeding the AC-bus. By dividing the power system in different parts the system becomes more robust concerning faults.

The main power source can in this case be a generator set driven by a combustion engine which runs on diesel or heavy oil. The efficiency of a medium speed diesel motor is continuously improved and the present values of consumption are less than 200 grams of fuel per kWh for an optimal working pointb(4). This is regarded as high efficiency, but only around 40 percent of the energy is used. This leads to the thought that there can be alternative ways to store and utilize energy in such power systems. Storing electric power is an accelerating technology, and the energy density of a battery is growing. New hybrid solutions is becoming more common, as pollution and green solutions become more attractive and reliable. The advantage of having a hybrid power system is the possibility to store and deliver energy, and having a fast time response (5). It is under certain circumstances possible to have an energy storage device, such as batteries, capacitors flywheels etc, as a backup generator (6).

The concept of electric propulsion is not new. There are several advantages for using electricity as a energy source on a marine vessel. The reduction in life cycle cost due to the reduced fuel consumption and maintenance, increased redundancy to single failure in system, possibility to optimize prime movers etc.

Because of the generators being synchronous machines, the power system can handle sudden changes in load because of the inertia the synchronous machines deliverers. When the generators are powered down, and the grid is supposed to be run by the batteries only, the inertia delivered by the synchronous machines are not available. When there are sudden load changes this can lead to a dip in frequency and voltage, leading to a more uncertain source of power. By implementing mathematical models of a synchronous machines in the control system for the inverters inverting the DC-voltage from the

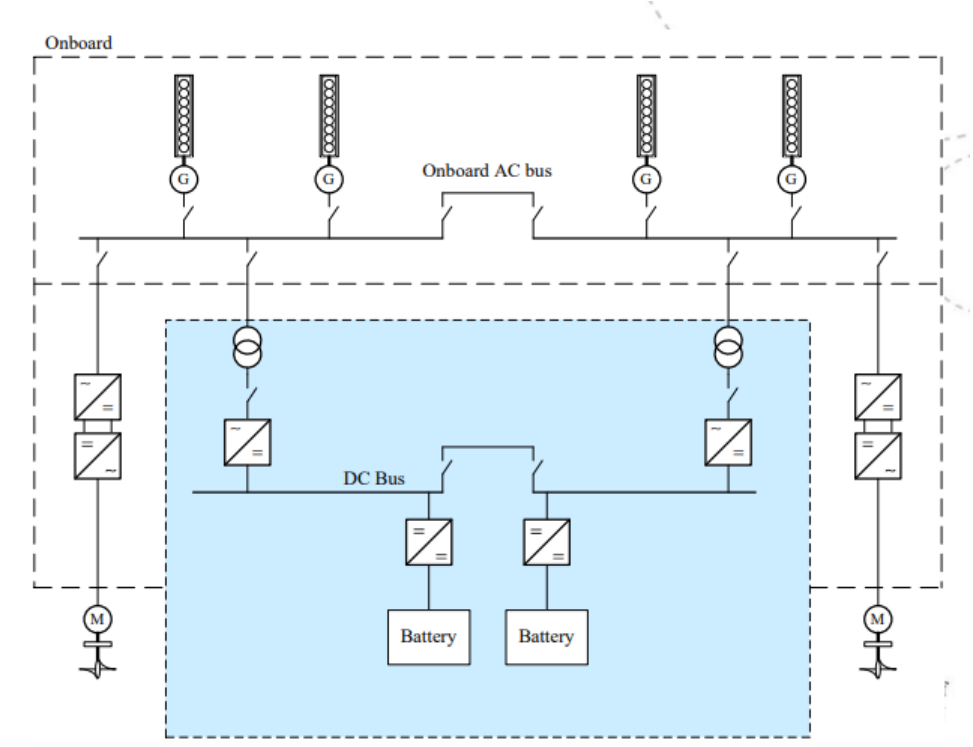

Figure 1: Overview of a possible topology for a hybrid power system on a marine vessel.

batteries, this problem can be solved in different ways in order to ensure a more reliable and secure source of power.

The main consumers of energy on a marine vessel is the machines operating the propellers. Dependent on the size and specifications on the ship, these will be relatively big, with second order load characteristics.

2.2 Virtual synchronous machine

The concept of Virtual synchronous machines, then called VISMA, was introduced in 2007 by Beck and Hesse (7). This described a new type of inverter control, with inverters operating with a storage system for energy, having the same amount of inertia and damping properties as an electromechanical synchronous machine (8). After this there was developed several approaches for adding virtual inertia to electronic power converters. Due to the many possible ways to model a SM, there exists many different solutions for emulating inertia. Varying in complexity and detail, different mathematical models can give a more detailed solution, but the trade off is the computational power required to solve these models (2). In this case the best design suited for modeling is not necessarily the most complex.

For several reasons it can be desirable to switch between power sources in order to reduce fuel consumption and limit the pollution for a marine vessel. This is could be done by implementing a battery storage system able to deliver and supply power to the grid. It would be desirable to run the power system hybrid, reducing the power demand of the generators driven by fuel, making the total amount of fossil fuel reduced. This means that the power gird should be able to have multiple operating conditions. There are many solutions for realizing such a feature. For operations of inverters in parallel

with a SM or something with swing mass, a PLL can be used in order to synchronize the frequency of the voltage. When the system should be run by the inverters alone, a PLL is not suitable and the inverters need to control the voltage. This could be solved by introducing a master-slave topology, where one of the inverters controls the frequency and others synchronize to the master. Then the problem with redundancy arises. If the master fails, there needs to be a backup to ensure a reliable power delivery. By implementing VSM this problem simplifies because by implementing the traits a SM gives to the power grid in the control structure of the inverter, the inverters can seamlessly switch between operating conditions. This switch can be done without changing the control system for the inverters and is one of the benefits of implementing a VSM control structure.

The system model can be split in to two main parts as illustrated in figure 2. First we have the conventional part with the inverter, LC-filter, grid current controller and measurement processing. The inverter is receives a PWM signal in the abc-frame controlled by the current controller. The measurement processing transforms everything to the dq-coordinate system, with the phase voltage a in abc frame aligned with the d-vector in dq-coordinates. The second part of this system is the VSM model. This consists of an electrical model, and model for emulating the inertia. Im addtion a automatic volgate regulator (AVR) and a Governor is implemented. An advantage of the VSM is the possibility to have this intuitive physical interpretation which is somewhat analog to the modeling of SM. (9)

Because of the switching in the inverter, noise can be transmitted to the AC-grid. To avoid this, an LC-filter is implemented to smooth out the voltages. Because of the nature of electrical impedance of an capacitor and an inductor, setting the capacitance in parallel to ground and the inductor in series will remove high frequency components out from the inverter.

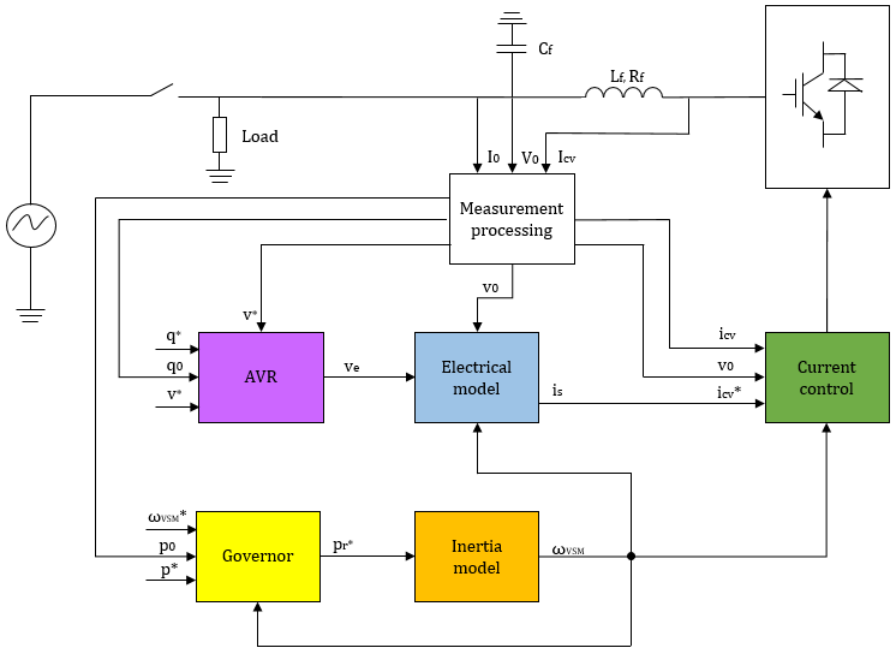

Figure 2: System model showing The VSM based control of the inverter.

2.2.1 Emulating inertia

The key of the VSM control structure implementation is the active power control and the control of the power balance based on the grid synchronization. This ensures the inertia behavior for the VSM.

There are several ways to implement a SM in an inverter. Since a VSM is implementing a SM in a control scheme, it contains a mathematical model for a synchronous machine. This means that if the VSM is supposed to mimic a SM at a great accuracy, a full order model of a SM should be used. But a full order model is unnecessary because it implements more than needed complexity to the system, and makes it hard to realize (10).

The method considered is this thesis is the swing equation used for a VSM(2). This is a natural choice if the desired effect is to emulate inertia and damping. The equation is given in 1. This equation contains the mechanical and the electrical part of a SM. The electrical part is based on the stator voltage equation. This equation describes the relationship between the stator and voltage current. T_{el} represents the electromagnetic torque, T_0 is the mechanical torque, ω the rotating speed of the machine, ω_g is the angular frequency of the grid, J is the inertia of the rotor and D is a coefficient that represents the damping torque associated with the damper windings during transient responses. Since D is a variable for a SM, this model cannot give the same performances as SM in the full operating range.

$$T_{el} - T_0 = D(\omega - \omega_g) + J\frac{d\omega}{dt} \tag{1}$$

The swing equation can be rewritten using the fact that $P = T\omega$, the equation 1 can be rewritten and transformed to the frequency domain as 2. Here the assumption of small perturbations in order to make the equation valid.

$$P_{el} - P_0 \approx K_d(\omega - \omega_g) + J\omega_g s\omega \tag{2}$$

Then by introducing a time constant $T_a = 2H$ the equation can be rewritten in per unit values as

$$p_{el} - p_0 \approx k_d(\omega_{pu} - \omega_{g,pu}) + T_a s\omega_{pu} \tag{3}$$

An alternative method is to emulate an estimatine of the the power response. By rewriting equation 3 and taking in $\omega_{g,pu}$ addition to p_{el} as a reference, the power delivered from the inverterter can be estimated.

$$p^*_{el} = p_0 + k_\omega(\omega^*_{g,pu} - \omega_{g,pu}) + k_i s\omega_{g,pu} \tag{4}$$

The constants k_ω and k_i is introduced. k_ω is replacing the damping constant K_d. k_ω is here a steady state droop constant, and k_i replaces T_a which is the inertia constant. This method requires that the inverter is able to control power can be controlled by the inverter. $\omega_{g,pu}$ is estimated using the grid frequency. This means that the model is dependent on the frequency of the grid, and is measured with an PLL. Because of this and the fact that this model does not give a virtual inertia and therefore is dependent on a physical inertia to work, it is not a suitable method.

The method used in this thesis was the linearized swing equation shown in equation 4. It was implemented as:

$$\omega_{VSM} = \frac{1}{T_a s}(p^{r*} - p_0 - k_d(\omega_{VSM} - \frac{\omega_d}{s + \omega_d}\omega_{VSM})) \tag{5}$$

Here T_a is the machanical time constant, p^{r*} is the virtual inertia instant power rotating the inertia, p_0 is the power measured after the LC filter. ω_{VSM} and ω_b is the angular per unit speed of the inertia

and the per unit base frequency. θ_{VSM} is the position of the rotating frame, and is used in the SRRF transformations.

Here a high pass filter is implemented in order to include the damping. If there were enough inertia in the grid, the frequency would be measured and a deviation in the frequency of the inverter and the grid could be calculated. Instead of using measurements, a high pass filter is implemented instead such that a change in frequency would resemble the behavior of the error of a reference value and a measured value. This assumption can be made since both signals will be around 1 pu. The implementation is done using a low pass filter and removing the low frequency components from ω_{VSM}. This will produce a damping similar to a SM, if the grid frequency changes relatively slowly compared to the VSM speed.

From the equation for the inertia emulation it can be shown that a droop controller for active is equivalent to each other. In figure 3 the topology for a active power droop controller is shown.

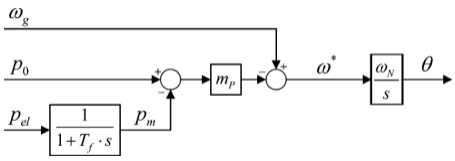

Figure 3: Droop controller active power control.

From the block chart the equations can be written as:

$$p_{el} = (1 + T_F \cdot s)(\frac{1}{m_p}(\omega_g - \omega^*) + p_0) \tag{6}$$

By expanding the expression one can write

$$T_f \frac{1}{m_p} s \cdot \omega^* = p_0 - p_{el} - \frac{1}{m_p}(\omega^* - \omega_g) \tag{7}$$

Comparing this with the equation for emulating inertia, it can be observed that both have power and frequency inputs, and provide a phase angle of the voltage based on the frequency droop. Here the assumptions constant set points for ω_g and p_0, and steady state for the system is done. Comparing to equation 7 the swing equation:

$$p^*_{el} = p_0 + k_\omega(\omega^*_{g,pu} - \omega_{g,pu}) + T_a s \omega_{g,pu} \tag{8}$$

By observing the equation for emulating inertia and the equation for the active power droop controller, the similarity is that $T_a = T_f \frac{1}{m_p}$ and $k_d = \frac{1}{m_p}$. This means that the droop gain m_p is the inverse of the damping gain k_d in the VSM. The time constant T_a serves as a low pass filter on the active power measurement as it does for the virtual inertia.

2.2.2 Electrical model

In order to make the inverter behave like a SM a mathematical model is implemented. The electrical model calculates a virtual stator current, i_s, numerically by simulating the model. These currents are then directed to synchronous reference frame (SRF)-current controllers. The model is shown in 10, where i_s, v_0 and i_s are complex values. r_s and l_s are the virtual stator impedance, ω_b is the base frequency, and finally ω_{VSM} is the virtual speed of the inertia in per unit values. $\mathbf{v}_e$ represents

the internally induced voltage in the SM. Since the d-axis of the SRF is used as the reference in the transformation, v_e is aligned with this axis. Everything is represented in this synchronously rotating reference frame such that the d-axis component is represented as real values and q-axis as imaginary perpendicular to the d-axis. The transient and subtransient of the equation is not included as a part of the equation. This is because it is not necessary to model the VSM characteristics to an exact match to a SM. Because it is a virtual control scheme only the beneficial characteristics is emulated. The same goes for the whole design as well; parameters is not necessarily bonded by physical constraints and the tradeoffs done when designing a SM needs no thought.

For modeling the SM the following RL-curciut used as the equivalent.

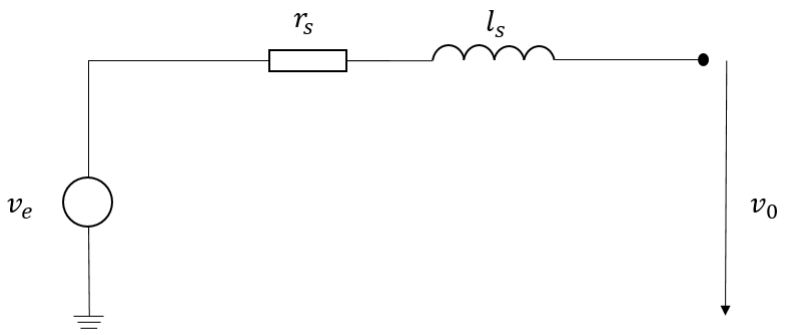

Figure 4: Simplified equvalence circuit for the stator on a SM.

Voltage balance gives

$$\mathbf{V}_e^{\alpha\beta} = \mathbf{I}_s^{\alpha\beta} r_s + r_s \frac{d}{dt} \mathbf{I}_s^{\alpha\beta} \tag{9}$$

Writing in pu and transforming to dq-frame gives:

$$\frac{d\mathbf{i}_s^{dq}}{dt} = \frac{\omega_b}{l_s}\mathbf{v}_e^{dq} - \frac{\omega_b}{l_s}\mathbf{v}_0^{dq} - (\frac{r_s\omega_b}{l_s} + j\omega_{VSM}\omega_b)\mathbf{i}_s^{dq} \tag{10}$$

Here $\mathbf{i}_s$ is the virtual stator current, ω_b is the base frequency in per unit value while, ω_{VSM} is the per unit speed of the virtual inertia. r_s and l_s are the virtual stator resistance and inductance, and are free variables in terms of tuning. Changing r_s and l_s values will influence the system response.

A alternative approach to modeling the electrical model for the SM is using a algebraic representation of the stator currents. This can be illustrated as a phasor diagram as seen in 5. By observing the equations, one can see that this is method is equivalent to the stationary solution for the model introduced earlier, and is therefore called a quasi-stationary model.

In figure 5, E is the induced voltage and V_g is the terminal voltage. The d-axis is directed along the generators phase voltage, and the q-axis is orthogonal to the d-axis. The angle between V_g and E is δ, the angle used for PLL synchronization(11).

$$\boldsymbol{i}_s = \frac{\boldsymbol{v}_e - \boldsymbol{v}_0}{(r_s + j\omega_{VSM} l_s)} \tag{11}$$

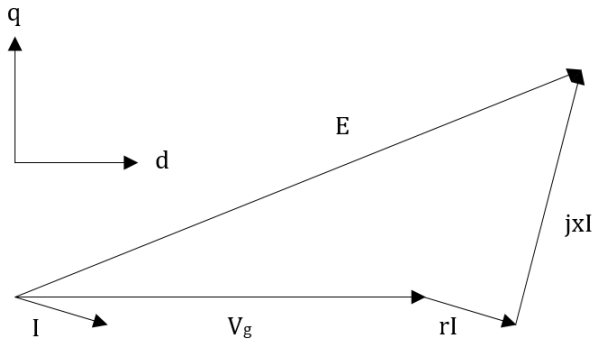

Figure 5: Phasor diagram for a generator.

Due to oscillatory behavior at the measurement at v_0, it is necessary to include a low pass filter to ensure stable operation. This means that both methods becomes first order differential equations due to implementation of the low pass filter. The dynamical model first introduced is more widely used rather than the quasi stationary and will therefore be the method used in this thesis.

2.2.3 Automatic voltage regulator and Governor

The voltage controller controls the amplitude of the induced voltage v_e of the virtual synchronous machine model. It consists of a droop-controller of the reactive power in series with a PI controller for controlling v_e. In the droop-controller the measurement for q is low pass filtered and and subtracted to the reference. The gain k_q controls the droop function in the voltage reference. It gains the difference between the low pass filtered between the measured and a set point of reactive power. Here the set point defines the amount of reactive power for when the droop effect of the voltage value changes from positive to negative. The output of the voltage v_e can be written as

$$\hat{v_e} = (K_{pv} + \frac{K_{iv}}{s})(K_q(q^* - \frac{\omega_{qf}}{s + \omega_{qf}}) + \hat{v^*} - \hat{v_0}) \tag{12}$$

The governor controls the frequency of the inverter and gives the reference value of the active power. As in the AVR, there is a droop controller implemented. Here the active power is reference is given by a external reference summed up with the droop controller.

$$p^{r*} = p^* + k_\omega(\omega^*_{VSM} - \omega_{VSM}) \tag{13}$$

2.3 Synchronous reference frame current controller

Using the electrical model to create a reference signal for the i_{dq} currents, various controllers can be used.
Synchronous reference frame (SRF) current controller is implemented. By using a voltage balance of the input of the inverter and the filter, the following expreisson can be deduced:

$$\boldsymbol{V}_c^{\alpha\beta} = \boldsymbol{V}_f^{\alpha\beta} + R_l\boldsymbol{I}_c^{\alpha\beta} + L\frac{d}{dt}\boldsymbol{I}_c^{\alpha\beta} \tag{14}$$

The SRF-current controller utilizes a PI-controller in order to reach its reference. Since the reference signal is DC-components, the control system should not have any steady state errors. In order to

simplify the model there is introduced decoupling terms. By doing this the system becomes a SISO system instead of a MIMO system. These terms is implemented as feed forward terms, and the resulting equations is reduced to:

$$\underbrace{v_{d,PI} + v_{0,d} - \omega_{pu} \cdot i_{c,q}}_{v_{c,d}} = v_{f,d} + r_f i_{c,d} + \frac{l_f}{\omega_b} \frac{d}{dt} i_{c,d} - \omega_{pu} l_f \cdot i_{c,q} \tag{15}$$

$$\underbrace{v_{q,PI} + v_{0,q} + \omega_{pu} \cdot i_{c,d}}_{v_{c,q}} = v_{f,q} + r_f i_{c,q} + \frac{l_f}{\omega_b} \frac{d}{dt} i_{c,q} + \omega_{pu} l_f \cdot i_{c,d} \tag{16}$$

$$v_{d,PI} = r_f i_{c,d} + \frac{l_f}{\omega_b} \frac{d}{dt} i_{c,d} \tag{17}$$

$$v_{q,PI} = r_f i_{c,q} + \frac{l_f}{\omega_b} \frac{d}{dt} i_{c,q} \tag{18}$$

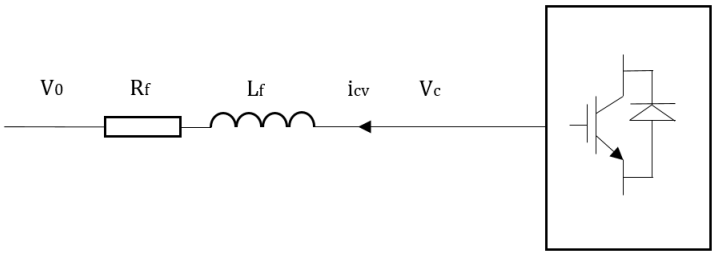

Figure 6: Inverter in series with filter delivering power to a grid.

The tuning parameters of the PI-controllers in the SRF-current controller can be found by examining the transfer funtion of the inner control loop, and is shown in the next chapter.

3 Methodology

This chapter goes through the implementation of the model in simulink. Block charts, equations and a state space representation is included. In the end of this chapter the system equations is presented.

3.1 Modeling conventions

For calculating the active and reactive power calculations for the AVR and Governor, the following relationship is used:

$$p_0 = v_{0,d} \cdot i_{o,d} + v_{0,q} \cdot i_{o,q} \tag{19a}$$

$$q_0 = -v_{0,d} \cdot i_{o,q} + v_{0,q} \cdot i_{o,d} \tag{19b}$$

Using the measured voltage components the voltage amplitude $\hat{v}_0$ used in the voltage controller is calculated as:

$$\hat{v}_0 = \sqrt{v_{o,d}^2 + v_{o,q}^2} \tag{20}$$

The Park-transform used in order to transform measurements from the abc-frame to the dq-frame is a power variant a-phase to d-axis alignment with the following transformations matrix:

$$\begin{bmatrix} d \\ q \\ 0 \end{bmatrix} = \begin{bmatrix} cos(\theta) & cos(\theta - \frac{2\pi}{3}) & cos(\theta + \frac{2\pi}{3}) \\ -sin(\theta) & -sin(\theta - \frac{2\pi}{3}) & -sin(\theta + \frac{2\pi}{3}) \\ \frac{1}{2} & \frac{1}{2} & \frac{1}{2} \end{bmatrix} \begin{bmatrix} a \\ b \\ c \end{bmatrix} \tag{21}$$

3.2 Implementation

The system model is modeled in Simulink. In addition to the converter and the SM, a synchronous machine and a load is modeled. This is in order to achieve a model similar to a ship power system. The purpose is to simulate how and observe how the system reacts to sudden changes of the distribution of how the system delivers to a load.

3.2.1 SRF Current controller

The gains inside the PI-controllers used in the current controller, Kp and Ki, needs to be found. Using the equation 15 the open loop transfer function of the SISO system can be seen in equation 22. Starting with examining the open loop transfer function, $h_{OL,cc,dq}(s) = \frac{i_{c,dq}(s)}{v_{PI,dq}(s)}$. By choosing $T_{ic} = T_1$ the pole from the dominant time constant is removed (the filter inductor time constant), according to modulus optimum. (12)

$$h_{OL,cc,dq}(s) = \frac{i_{c,dq}(s)}{v_{PI,dq}(s)} \approx \underbrace{K_{p,cc}\frac{1 + T_{1,c}s}{T_1 s}}_{PI-controller} \quad \underbrace{\frac{1}{T_{sum}}}_{Delayapprox.} \quad \underbrace{\frac{1}{r_1}\frac{1}{T_1}}_{Filterinductor} \tag{22}$$

$$T_{i,c} = T_1 \tag{23}$$

$$h_{OL,cc,dq}(s) = \frac{i_{c,dq}(s)}{v_{PI,dq}(s)} \approx \frac{K_{p,cc}}{r_1 T_1 s}\frac{1}{1 + T_{sum}s} \tag{24}$$

When closing the loop, the gain $K_{p,cc}$ can be calculated.The gain is found in order to achieve critical damping. From the harmonic oscillator this is $\delta = \frac{1}{\sqrt{2}}$. This gives a gain

$$K_{p,cc} = \frac{r_1 T_1}{2T_{sum}} = \frac{l_1}{4\pi T_{sum}} \tag{25}$$

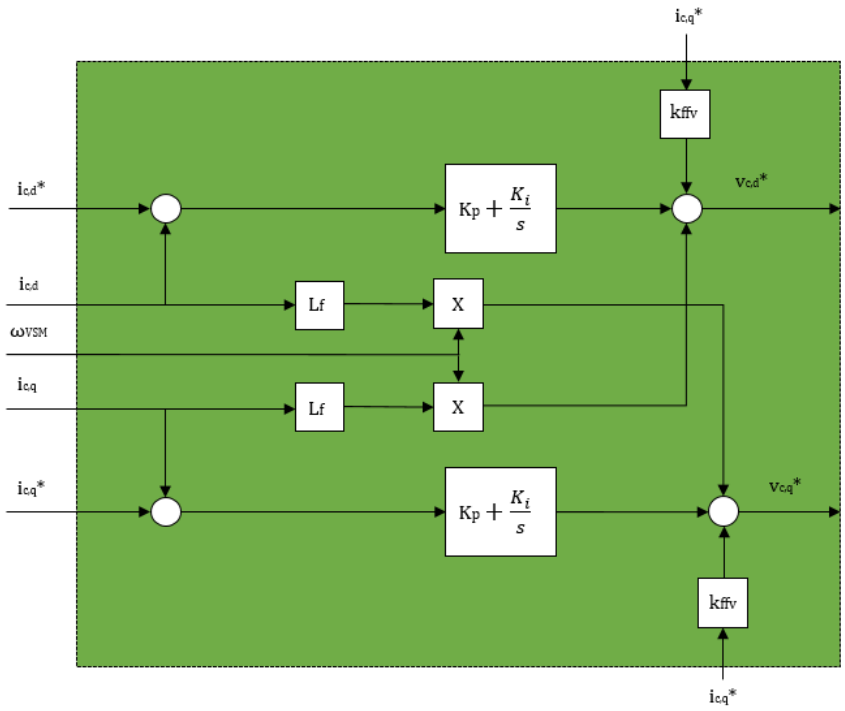

Figure 7: SRF current controller.

3.2.2 Inertia model and governor

By observing the swing equation, it can be seen that the grid frequency is used as a feedback error for damping the response. Since this analysis is considering steady state, it is assumed that the frequency ω_{VSM} have small deviations from the grid frequency. By high pass filtering the frequency of the VSM and multiplying it with the damping coefficient K_d, it is possible to achieve an approximate effect as if the grid frequency was used (1).

The high pass filter is implemented as a feed forward low pass filter as seen in figure 9. The cut off frequency, ω_D, for this filter set to $5rad/s$. For a SM the mechanical time constant is two times the inertia constant($2H$), and is here 4 seconds. By using a wrapped integrator in Matlab, the phase angle for the VSM (θ_{VSM}) is calculated taking the derivative of ω_{VSM}. This gives a saw-tooth like signal, used for the dq-transformations.

The closed loop transfer function for the inertia model can be written as:

$$h_{cl} = \frac{\omega}{p}(s) = \frac{s + v_d}{T_a s^2 + (K_d + T_a\omega_d)s + 2K_d\omega_d} \tag{26}$$

Using this equation, the poles can be placed such that the inertia behaves in a desirable way. Inserting the parameters used in the simulations results in two negative real values, implying stability when only looking at the inertia transfer function.

As shown in the figure 9, the state κ is introduced, and is defined as the output of the low pass filter. This is in order to simplify the expression and make it possible to write the system on state space form. This is not done in this thesis but is a possible future work.

$$\frac{d\omega_{VSM}}{dt} = \frac{p^{r*}}{T_a} - \frac{p_0}{T_a} - \frac{k_d(\omega_{VSM} - \kappa)}{T_a} \tag{27a}$$

$$\frac{d\kappa}{dt} = \omega_d \omega_{VSM} - \omega_d \kappa \tag{27b}$$

$$\frac{d\theta_{VSM}}{dt} = \omega_{VSM} \omega_b \tag{27c}$$

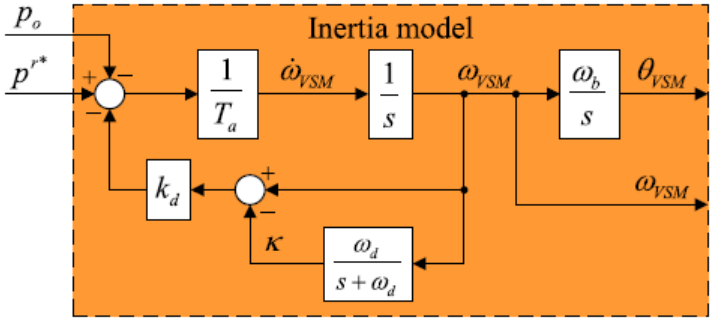

Figure 8: Inertia model.(10)

The equation for the governor is implemented as the equation from chapter 2.

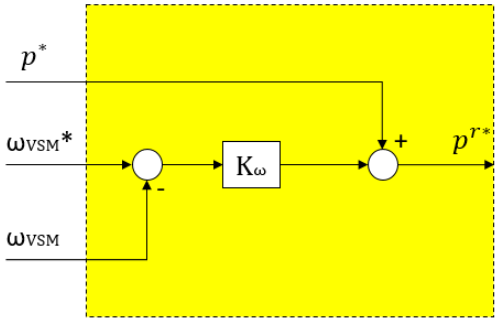

Figure 9: Governor, introducing frequency droop.

3.2.3 Electrical model

In the electrical model there is two parameters that can be tuned for the best possible behavior of the electrical model of the SM machine. r_s and l_d, which is the equivalent to the stator resistance and inductance of a real SM. These parameters influences the damping of the control system by either increasing the stator resistance or decreasing the stator inductance.

By using equations 28, the implementation of the model in Matlab/simulink, the model becomes as seen in figure 10.

$$\frac{di_{s,d}}{dt} = \frac{\omega_b}{l_s}(v_e - v_{0,d}) - \frac{r_s \omega_b}{l_s} i_{s,d} + \omega_{VSM} \omega_b i_{s,q} \tag{28a}$$

$$\frac{di_{s,q}}{dt} = \frac{\omega_b}{l_s} v_{0,q} - \frac{r_s \omega_b}{l_s} i_{s,q} - \omega_{VSM} \omega_b i_{s,d} \tag{28b}$$

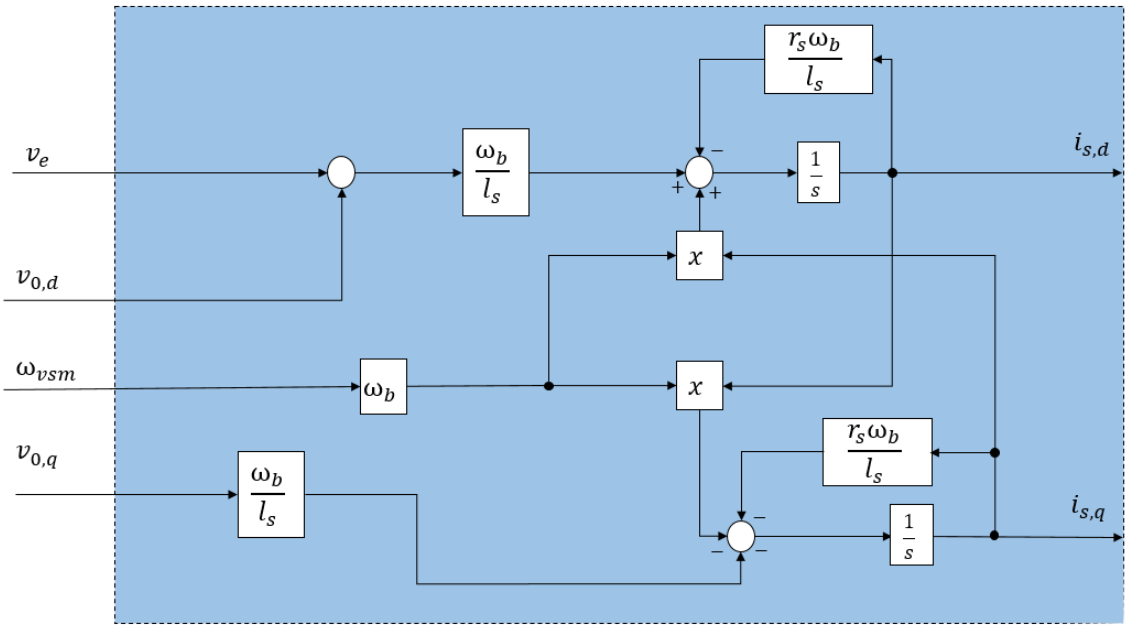

Figure 10: Electrical model.

3.2.4 Voltage control

For controlling the amplitude of the voltage at the capacitors of the LC-filter, v_0, a controller is used giving a reference for the virtual induced voltage, $\hat{v_e}$. From figure 11 the equations 12 is implemented. As mentioned in earlier, a PI-controller is used for controlling the reference. The droop gain is set to 0.1. The reactive power measured, q_0, must be low pass filtered. This is necessary for rejecting noise and disturbances, giving a more stable control loop.

The voltage controller is cascaded with the current controller, controlling the induced voltage, and changing the reference of the current controller. Since the system consists of multiple control loops, the natural frequency for the outer loop must be 10 at least times slower for the natural frequency for the inner loop.(13). The gains k_{pv} and k_{iv} was approximated using Ziegler-Nichols method for finding parameters for the PI-controller, giving a response that works. This is not a optimal solution, but give a working model.

In order to simplify the expression from chapter 2.2.3 and make it possible to state space transform, the state ζ and q_m is introduced. The two states represents the integrator state of the PI-controller and low pass filtered reactive power, respectively. The new equation becomes:

$$\hat{v_e} = k_{pv}(\hat{v}^* - \hat{v}_0) + k_{pv}k_q(q^* - q_m) + k_{iv} \tag{29}$$

$$v_{c,d} = v_{f,d} + r_1 i_{c,d} + \frac{l_1}{\omega_b}\frac{d}{dt} i_{c,d} + j\omega_{pu} l_1 i_{c,q} \tag{30}$$

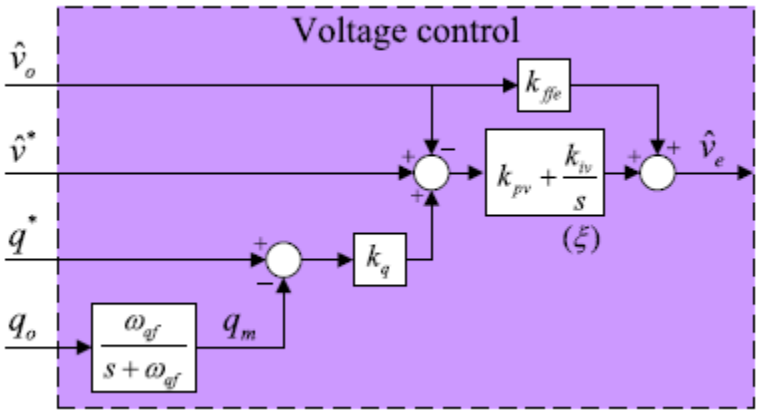

Figure 11: Voltage controller.

3.3 System equations

Below, the system equations for the model is presented. This model is done similar to (1) and (8). A state space model is not presented in this thesis, but is a future work.

The voltage after the filter, $\frac{dv_0}{dt}$, can be found by summation of the voltages at the filter, and transforming from $\alpha\beta$ to dq. The equation for $\dot{v_0}$ becomes:

$$\frac{dv_{o,d}}{dt} = \omega_b \omega_{VSM} v_{0,q} + \frac{\omega_b}{c_f}(i_{cv,d} - i_{o,d}) \tag{31a}$$

$$\frac{dv_{o,q}}{dt} = -\omega_b \omega_{VSM} v_{0,d} + \frac{\omega_b}{c_f}(i_{cv,q} - i_{o,q}) \tag{31b}$$

For finding the equation for the current from the inverter, $\frac{di_{cv}}{dt}$, the feed back loop to the current controller is used. This leads to the following expression:

$$\frac{di_{cv,d}}{dt} = -\frac{\omega_b}{l_f} v_{0,d} - \frac{\omega_b(k_{pc} + r_f)}{l_f} i_{cv,d} + \frac{\omega_b k_{ic}}{l_f}\gamma_d + \frac{\omega_b k_{pc}}{l_f} i_{s,d} \tag{32a}$$

$$\frac{di_{cv,q}}{dt} = -\frac{\omega_b}{l_f} v_{0,q} - \frac{\omega_b(k_{pc} + r_f)}{l_f} i_{cv,q} + \frac{\omega_b k_{ic}}{l_f}\gamma_q + \frac{\omega_b k_{pc}}{l_f} i_{s,q} \tag{32b}$$

Here the state γ is introduced to simplify the expression and possible to write on state space form. It represents the error of the reference and current value of icv in the current controller, and is defined as:

$$\frac{d\gamma_q}{dt} = -i_{cv,q} + i_{s,q} \tag{33a}$$

$$\frac{d\gamma_q}{dt} = -i_{cv,q} + i_{s,q} \tag{33b}$$

For expressing the voltage out of the filter, v_0, the state $\delta\theta_{VSM}$. This is in order to get the phase angle of the VSM inertia referred to the phase angle to the grid. It is defined as:

$$\delta\theta_{VSM} = \theta_{VSM} - \theta_g \tag{34}$$

Expressing the state v_o as interpretation of the phasor diagram seen in 5 for the SM is used. v_0 is the voltage division between the grid and the LC-filter for the inverter. If the induced voltage in the VSM is aligned with the dq-frame of the inverter the derivative of the angle between the grid and induced voltage of the VSM can be written as:

$$\dot{\delta\theta_{VSM}} = \omega_{VSM} - \omega_g \tag{35}$$

This gives the possibility to geometrically observe the phasor diagram mentioned above, and find the following context:

$$v_{0,d} = v_g cos(\delta\theta) \tag{36a}$$

$$v_{0,q} = v_g sin(\delta\theta) \tag{36b}$$

Summation of voltage gives the expression for $\frac{di_0}{dt}$ and can be written as:

$$\mathbf{V}_0 - \mathbf{V}_g = R\mathbf{I}_0 + j\omega L_g \mathbf{I}_0 + L_g \frac{dI}{dt} \tag{37}$$

Transforming to dq-coordinates and inserting the expressions for v_0 gives:

$$\frac{di_{0,d}}{dt} = \frac{\omega_b}{l_g} v_{0,d} - \frac{\omega_b r_g}{l_g} i_{0,d} + \omega_b \omega_{VSM} i_{0,q} - \frac{\omega_b}{l_g} \hat{v_{g,d}} cos(\delta\theta_{VSM}) - \frac{\omega_b}{l_g} \hat{v_{g,q}} sin(\delta\theta_{VSM}) \tag{38a}$$

$$\frac{di_{0,q}}{dt} = \frac{\omega_b}{l_g} v_{0,q} - \frac{\omega_b r_g}{l_g} i_{0,q} + \omega_b \omega_{VSM} i_{0,d} - \frac{\omega_b}{l_g} \hat{v_{g,q}} cos(\delta\theta_{VSM}) - \frac{\omega_b}{l_g} \hat{v_{g,d}} sin(\delta\theta_{VSM}) \tag{38b}$$

The expression for the state ζ and q_m introduced in the AVR chapter, with ehe reactive power written as in chapter 3.1 becomes:

$$\frac{dq_m}{dt} = -i_{0,q} v_{0,d} \omega_{qf} + i_{0,d} v_{0,q} \omega_{qf} - q_m \omega_{qf} \tag{39a}$$

$$\frac{d\zeta}{dt} = -\sqrt{v_{0,d}^2 + v_{0,q}^2} - k_q q_m + k_q q^* + \hat{v}^* \tag{39b}$$

The currents in the virtual impedance is just as described in 10.

$$\frac{di_{s,d}}{dt} = \frac{\omega_b}{l_s}(v_e - v_{0,d}) - \frac{r_s \omega_b}{l_s} i_{s,d} + \omega_{VSM} \omega_b i_{s,q} \tag{40a}$$

$$\frac{di_{s,q}}{dt} = \frac{\omega_b}{l_s} v_{0,q} - \frac{r_s \omega_b}{l_s} i_{s,q} - \omega_{VSM} \omega_b i_{s,d} \tag{40b}$$

The resulting equations from the virtual inertia can be derived as:

$$\frac{d\omega_{VSM}}{dt} = -\frac{1}{T_a} i_{0,d} v_{0,d} - \frac{1}{T_a} i_{0,q} v_{0,q} - \frac{k_d + k_\omega}{T_a} \omega_{VSM} + \frac{k_d}{T_a} \kappa + \frac{k_\omega}{T_a} \omega_{VSM}^* \tag{41}$$

$$\frac{d\kappa}{dt} = \omega_d \omega_{VSM} - \omega_d \kappa \tag{42}$$

3.4 Testing the VSM

After building the model as described above, two loads and a SM was implemented to the system. One of the loads was modeled as a twelve-pulse rectefier, with an ideal current source on the DC-bus. This will be a constant and stable load, giving the opportunity to see how the VSM manages a sudden load change. The other load was a constant load, drawing a giver amount of power. The SM will represent the grid, as seen in figure 2. The test case for the VSM is that it runs parallel with a SM, delivering power to a load. The VSM and SM share the load at first but at a given time the SM will trip, and the VSM must deliver all power to the load by itself. This will test the stability and reliability of the VSM for handling a load without an inertia in the grid to rely on.

3.4.1 DC-source

In this paper there is not taken into consideration. This means that the DC-voltage source is modeled as an ideal source, and has no limitations on voltage or current.

3.4.2 Rectefier

The inverter model used is a built in function block in Matlab/Simulink called Two-Level converter, with the Average model mode. This function block implements switching by receiving a three phase voltage signal. This means that no PWM signal is needed and therefore not included in this paper.

4 Results

This chapter presents the results and explains the plots added. The results will be discussed in the next chapter.

The VSM model described above has been implemented in Simulink, and tested for different scenarios, checking and validating its functions. The model have been tested for delivering power to a stiff grid and to a SM. These two scenarios are relevant because the power grid for a marine vessel can be run with a diesel generator and/or connected to a land based power grid, which can be thought of as a stiff power grid with sufficient inertia. In addition, different scenarios have been simulated, such as load change, tripping of SM, changing in load distribution and going from a grid connection to a isolated grid with a SM and a VSM. The system was implemented as figure 12 shows. A load with value 1500 kW and 5000 Qvar inductive, and a twelve pulse rectifier drawing $750A$ DC have been implemented in order to test these scenarios. The rectifier has been implemented in order to test the model with harmonic distortion, as seen on the plotted results below. The model initialization is not included in any of the results for simplicity.

Parameter	Value	Parameter	Value
V_{LL}	690 V	k_{pc}	0.13
S_b	1.6 MVA	k_{ic}	11.8
ω_b	2π 50 Hz	k_{ffv}	0
v_g	1.0 pu	k_ω	20
ω_g	1.0 pu	k_{pv}	0.12
r_f	0.003 pu	k_{iv}	117.8
c_f	0.0074	ω_{qf}	200 rad/s
l_f	0.008	k_q	0.1
T_a	4 s	p^*	0.5 pu
k_d	40	q^*	0.0 pu
ω_d	5 rad/s	$\hat{v}^*$	1.0 pu
ω_d	0.25 pu	ω^*_{VSM}	1.0 pu

Table 1: Table showing the parameters used in the simulated model.

4.1 Testing with different damping parameters

Initially, the simulation was tested and compared to expected results. In figure 13 it can be seen the response of the frequency and active power, when a step change is done to the reference value of delivered power from the inverter. This was done in order to validate and test the virtual inertia implemented. The blue is T_a= 0.25 and K_d= 40, red T_a= 0.5 and K_d= 20 and yellow is T_a= 0.125 and K_d= 50.

4.2 Change of load

The system was tested with a change of load. This can be seen in figure 14, showing how the frequency is changed due to a load requiring more power, and 15 showing how the currents and the power is affected. The load that was added in addition to the initial load was 1 MW and a 5 kVA.

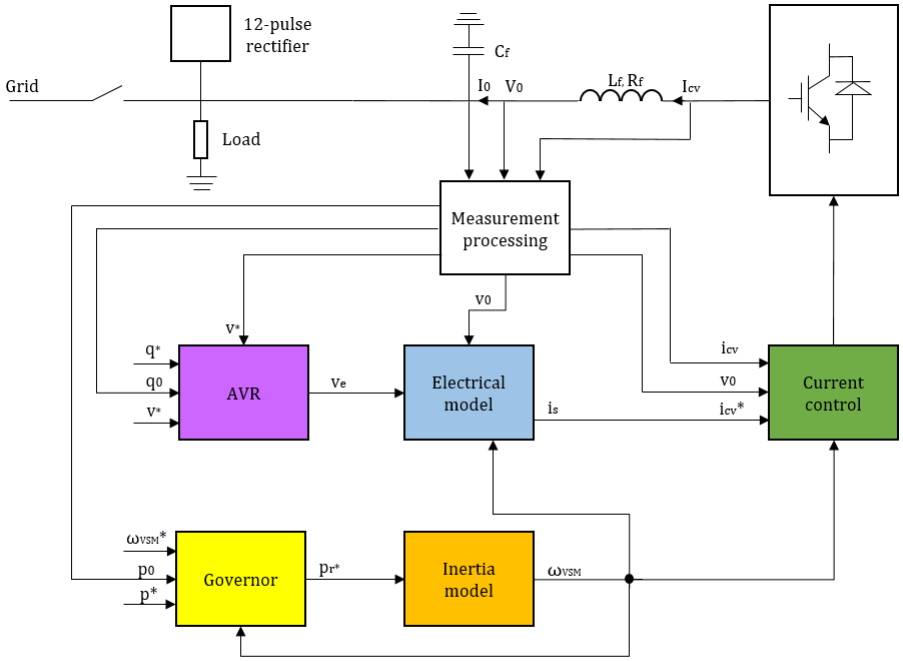

Figure 12: System model showing where the respective signals is measured.

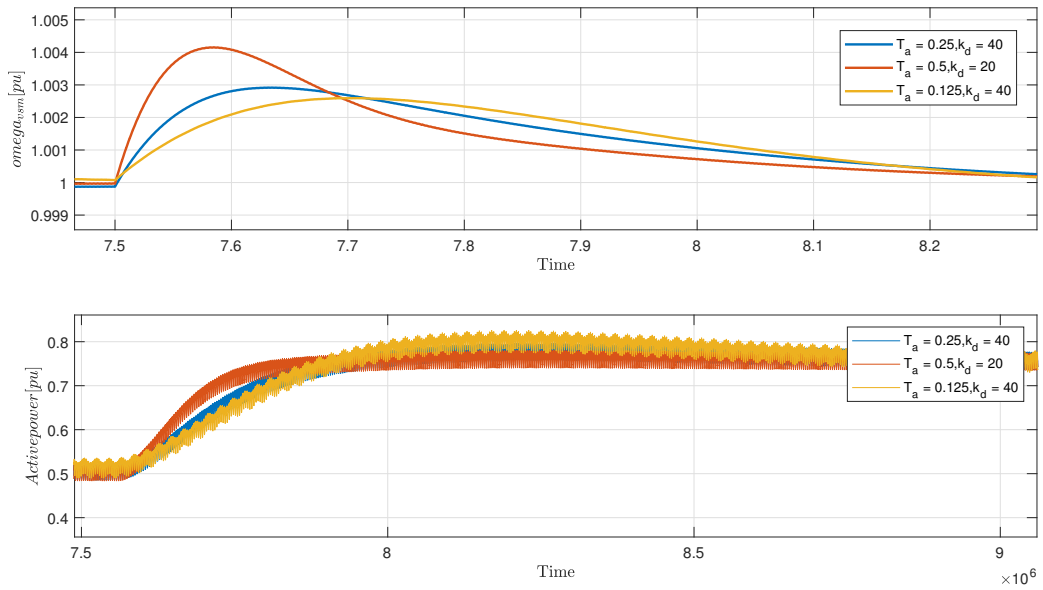

Figure 13: Plot showing the frequency and active power for different T_a and K_d. The blue is $T_a = 0.25$ and $K_d = 40$, red $T_a = 0.5$ and $K_d = 20$ and yellow is $T_a = 0.125$ and $K_d = 50$.

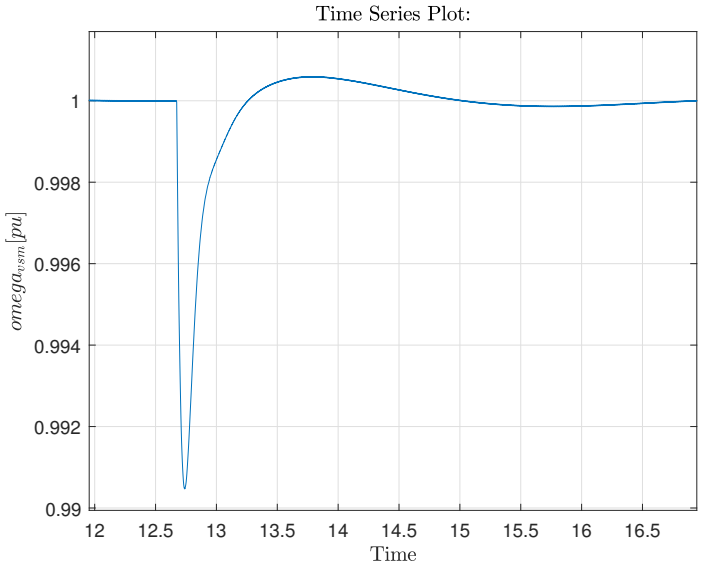

Figure 14: Plot showing the frequency when a load is added on the AC-line.

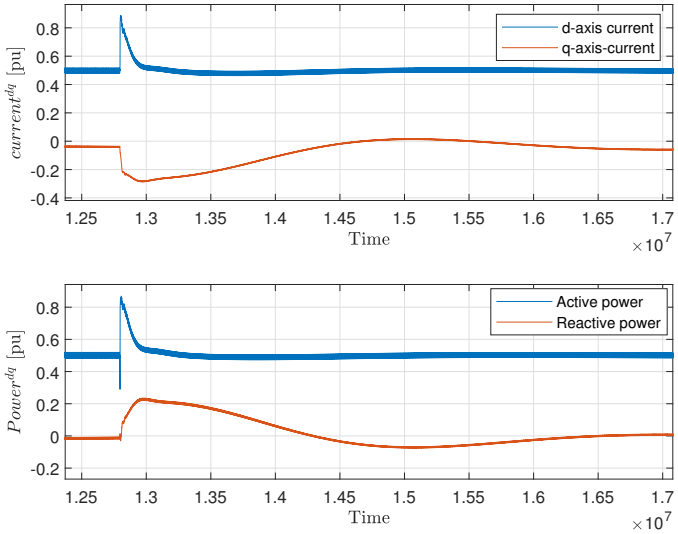

Figure 15: Plot showing the current and power delivered from the VSM, when a load is added to the system.

4.3 Tripping the connection of the SM

In figure 16 and 17 the results from tripping the SM in parallel to the VSM. The first figure shows how active and reactive power is changed, and the second shows the frequency. The set point was 0.75 pu for the inverter before the trip.

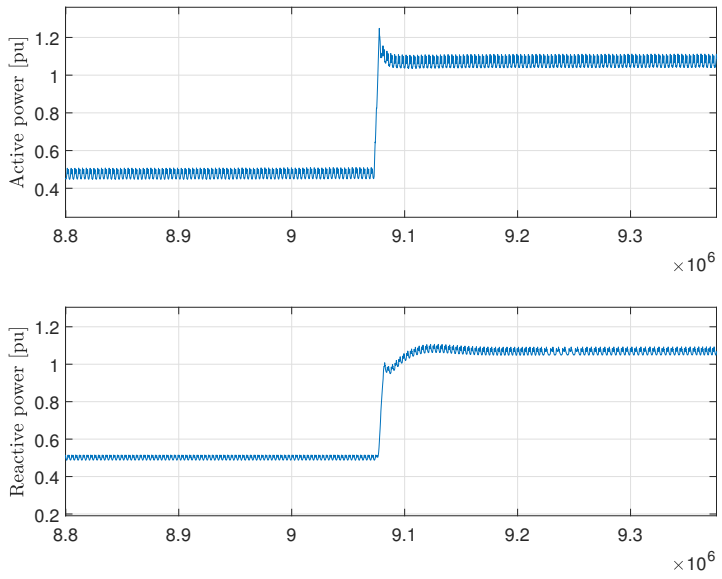

Figure 16: Plot of delivered power from the inverter when the SM trips.

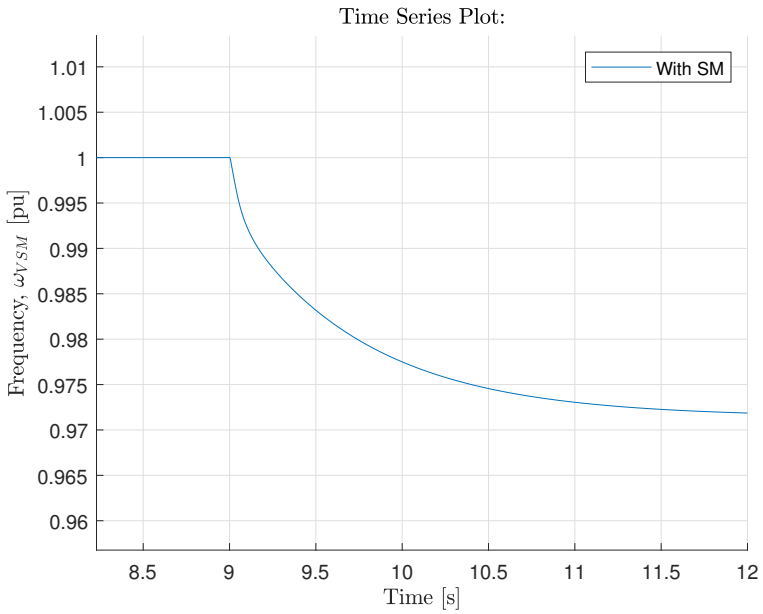

Figure 17: Plot showing how the frequency responds when tripping SM.

4.4 Tripping a islanded connection.

Here the system was initially connected to a grid, and when the system was in steady state the connection was broken. This led to the response seen in figure 18 and 19. These plots shows how the frequency and power changes.

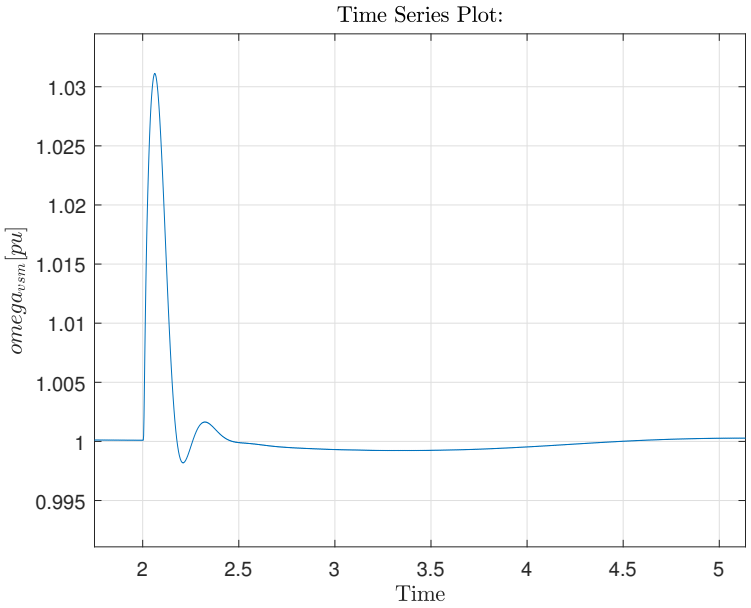

Figure 18: Plot showing the frequency when islanding

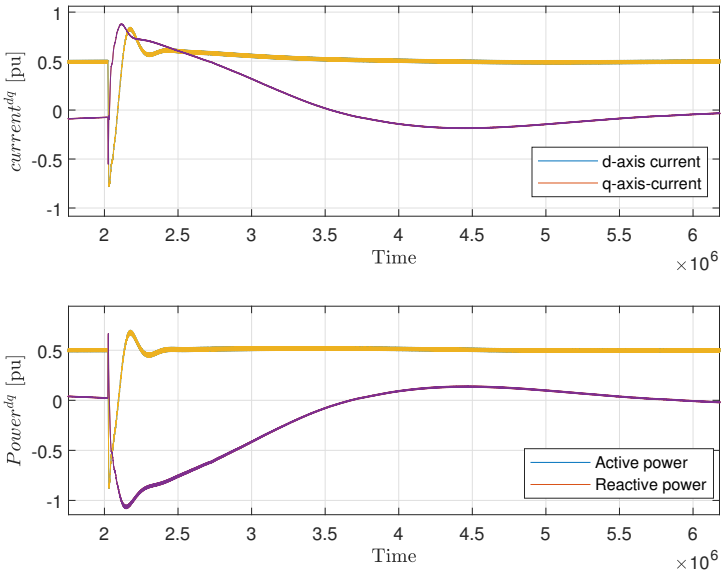

Figure 19: Plot showing the current and the power when islanding

5 Discussion

As mentioned in the previous part, the VSM have been simulated for various scenarios that are relevant for a marine power gird.

5.1 System model

The VSM-controlled inverter model has been implemented and simulated. The simulation results describes the outcome of the different scenarios tested, and describes the outcome of changing operation mode without changing the control structure. The model behaves stable and desirably for the different scenarios. The results highlights some of the benefits and perks of having a VSM control structure for an inverter delivering power to a grid.

However, the system model has some limitations. The model is not able to have a good initialization. This means that initially it cannot ensure a stable and reliable power grid when initializing. It needs a few seconds to reach steady state in order to achieve the results presented. Secondly, the DC-voltage source is modeled as an ideal voltage source. This means that the model does not consider the limitations a DC-voltage could have. It can be limited by how much power it can deliver, and the voltage level of the DC-side of the inverter can fall. A more detailed model of a marine power system is more than necessary for testing the VSM in detail with different things in consideration. This model is simplified to have two sources connected, a SM and a VSM, delivering to the marine power grid, except when an islanded connection is established.

5.2 Simulation results

The results from the simulations focuses on how the power flow from the VSM is, and how the frequency is controlled for the grid. The different scenarios are chosen because they are relevant for testing relevant aspects of a VSM. Even though this is a simplified model it can be representative for the possibilities of handling the problem when inertia in the power grid is weakened or not there at all.

5.2.1 Tuning of the VSM

A VSM have several degrees of freedom in terms of tuning, as mentioned above. Since it is supposed to mimic a SM, only the desired traits of a SM needs to be implemented, and is not constrained by physical limitations. This means that the inertia constant, T_a, can be chosen in order to give the VSM a desired behavior. Also the power losses due to the damping of does not come from an actual circuit but only appears in the control system. The damping coefficient, stator resistance and inductance are parameters that can be chosen in order to modify the behavior.

For checking these tuning parameters a step change in the active power reference was done when the grid frequency had stabilized in steady state 1 pu. Initially the active power reference was 0.5 pu, and was changed to 0.75 pu at a given time. This case is equivalent to a sudden increase in the input power og torque on the shaft of a SM.

Starting off with $T_a = 1/4$ and simulating the system with a SM in parallel, the response of the frequency seemed to be over-damped, see figure 13. By lowering the inertia constant, T_a, and the damping coefficient, k_d of the VSM, the system lost some of the damping. This figure also contains the resulting system response when the inertia constant and the damping coefficient were raised. The resulting behavior described in this figure can resemble the more damped response of a conventional SM. The active power have a ripple due to the 12-pulse rectifier drawing power from the grid. As the

damping goes the active power starts to oscillate more around its reference point. This is supressed when the damping coefficients is higher.

5.2.2 Change of load

A case relevant for a marine vessel is changes in the load of the system. During operation of a marine vessel, the loads drawing power from the grid can change, and it is important that the VSM is able to tolerate this. These loads can be propulsion units turning on, and the amount of power drawn can therefore be relatively big. Because of this, the system was tested with a step change in the load. This was modeled as an addition to the load in the circuit. A 1 MW and a 5 kVA load was added in parallel with the load already implemented. It was enabled with a switch, adding the load to the circuit at a given time. The set points for active and reactive effect delivered by the VSM were 0.5 pu and 0 pu, respectively. By observing figure 15, it can be seen that both the active and reactive effect experiences a disturbance, here the load, and then goes to steady state against the set points. This means that the additional load added to the system is managed by the SM in the system. This could be desirable if the energy source delivering on the DC side is a limited source with bounded delivery capacity. By having a constant set point for the VSM, the delivered power of the SM is indirectly controlled.

Even though the load is almost doubled, the frequency manages to stay fairly stable around 1 pu ω_{VSM}. As seen in figure 15, the VSM contributes to cover the sudden rise in the load, but the steadily go back to it's given reference values, 0.5 and 0.

5.2.3 Breaking the connection to a stiff grid

Being connected to a strong grid and suddenly disconnecting was tested. This test was done in steady state by tripping the grid connection. The figure 18 shows the frequency when tripping the grid connection. The system experiences a small dip in frequency, and then stabilizing relatively quickly.

This result shows a trait for implementing a VSM. The result shows that it is possible to seamlessly go to an islanded grid, being initially fed from a strong grid. A trait the VSM delivers to the grid is the possibility to go from a smooth and seamless transition to an isolated grid operation. This can be seen in figure 18 and figure 19. The system adapts to the sudden change and due to the emulated inertia the inverter manages to maintain stability. The power flow is immediately adapted to local load, instead of delivering effect to the grid.

5.2.4 Tripping a SM in parallel

A scenario for use of the VSM is when going from parallel power distribution, to single handed deliver all power itself. The model was run until it reached steady state, and at a given time the SM was tripped. This could be analog to a fault in the system causing the SM to be isolated from the grid. In figure 16 the power response can be seen. Here the set point was 0.75 pu for the inverter before the trip. As mentioned, the oscillations in power is because of the harmonic distortion created by the 12-pulse rectifier. In addition the plot of the frequency of the VSM can be seen in 17. When the inverter gets a sudden change in delivered power the frequency goes as expected down. This is because of the droop effect in the governor.
This test shows how the VSM handles one of its main objectives. By tripping the VSM the grids characteristics changes. After the SM is no longer connected it no longer has any swing mass giving inertia to the system. It shows that the emulated inertia works as intended, and no change in control system is needed.

6 Conclusion and further work

6.1 Conclusion

This project has studied some of the general capabilities of a VSM-controlled power converter, and have investigated methods for evaluating how a DC-source with VSM-based control can influence the stability and transient response of ship power system in various operating conditions. The VSM based control structure emulates inertia contributing to the total amount of inertia in the grid, and gives the possibility to operate in both grid and islanded connections without needing to change the control structure. A possible way to implement a VSM in a power grid, and simulated a model with different cases relevant for a marine power system have been explored and tested.

Seeing the simulation results, the VSM have fulfilled its main purpose, emulating inertia and giving the possibility to change sources delivering to the grid without having to change control structure or parameters. The inverter can deliver power to the grid without a utilizing a PLL for synchronization. It can handle changes in load and share the load in the system with other sources. As power systems for ships tends towards more electric solutions, VSM based control for an inverter is a efficient tool that can contribute to simplify this change.

6.2 Further work

For further work it would be possible to go into the model in more detail and do a stability and eigenvalue analysis. This would lead to a better understanding of the model, and give more insight in the possibilities in terms of tuning. All scenarios simulated have been about tripping something from the grid, but re-connecting have not been taken into consideration and can be a possible future work.

It would be relevant to investigate the outer control loop in more detail, along with the complete state space representation for a stability analysis of the inverter. The system equations presented in chapter 3 only yields for the inverter, a generator and the DC-source. A more comprehensive state space model could be presented, along with a comprehensive stability analysis.

Expanding the model and make it even more similar to a ship power system. In addition, a possibility is to test the systems handling of having too high load. What would happen if the controllers cannot reach the reference due to a limitation in the source of energy, or some other constraint limiting the system.

Designing an energy management system for a marine vessel utilizing VSM based control for inverters, could lead to an interesting case study. This could focus on optimizing the fuel usage, giving the opportunity to have a more stable load on the generators letting them work in the most efficient area.

References

[1] O. Mo, D'Arco, Salvatore, and J. A. Suul, J. A.Suul, "Evaluation of Virtual Synchronous Machines With Dynamic or Quasi-Stationary Machine Models," *IEEE Transactions on Industrial Electronics*, vol. 64, no. 7, 2017.

[2] D'arco Salvatore and Suul, "Virtual synchronous machines — Classification of implementations and analysis of equivalence to droop controllers for microgrids - IEEE Conference Publication,"

[3] E. Skjong, M. Molinas, E. Rødskar, and J. Cunningham, "The marine vessel's electrical power system: From its birth to present day," *Proceeding of the IEEE*, December 2015.

[4] A. K. Ådnanes, *Maritime Electrical Installations and Diesel Electric Propulsion.* ABB, 2003.

[5] M. Miyazakiand, A. Sørensen, and E. Pedersen, "Hybrid modeling of strategic loading of a marine hybrid power plant with experimental validation," November 2016.

[6] DNV-GL, "Rules for classification, part 6 additional class notations, chapter 2 propulsion, power generation and auxiliary systems," 2018.

[7] H. P. Beck and R. Hesse, "Virtual synchronous machine," *Electrical power quality and utilization*, 2007.

[8] B. Zhang, X. Yan, D. Li, X. Zhang, J. Han, and X. Xiao, "Stable operation and small-signal analysis of multiple parallel dg inverters based on a virtual synchronous generator scheme," *Energies*, vol. 11, p. 203, Jan. 2018.

[9] S. D'Arco, J. A. W. Suul, and O. B. Fosso, "A virtual synchronous machine implementation for distributed control of power transformers in smartgrids," 2015.

[10] D'Arco, Salvatore and Suul, J. A., "Equivalence of Virtual Synchronous Machines and Frequency-Droops for Converter-Based MicroGrids," *IEEE Transactions on Smart Grid*, vol. 5, pp. 394–395, Jan. 2014.

[11] Y. Hirase, K. Abe, K. Sugimoto, and Y. Shindo, "A grid-connected inverter with virtual synchronous generator model of algebraic type," *Electrical Engineering in Japan*, vol. 184, no. 4, pp. 10–21, 2013.

[12] R. Nilsen, *Electric Drives.* Department of Electric Power Engineering, 2018.

[13] T. I. Fossen, *Handbook of Marine Craft Hydrodynamics and Motion Control: Fossen/Handbook of Marine Craft Hydrodynamics and Motion Control.* Chichester, UK: John Wiley & Sons, Ltd, Apr. 2011.

7 Appendix

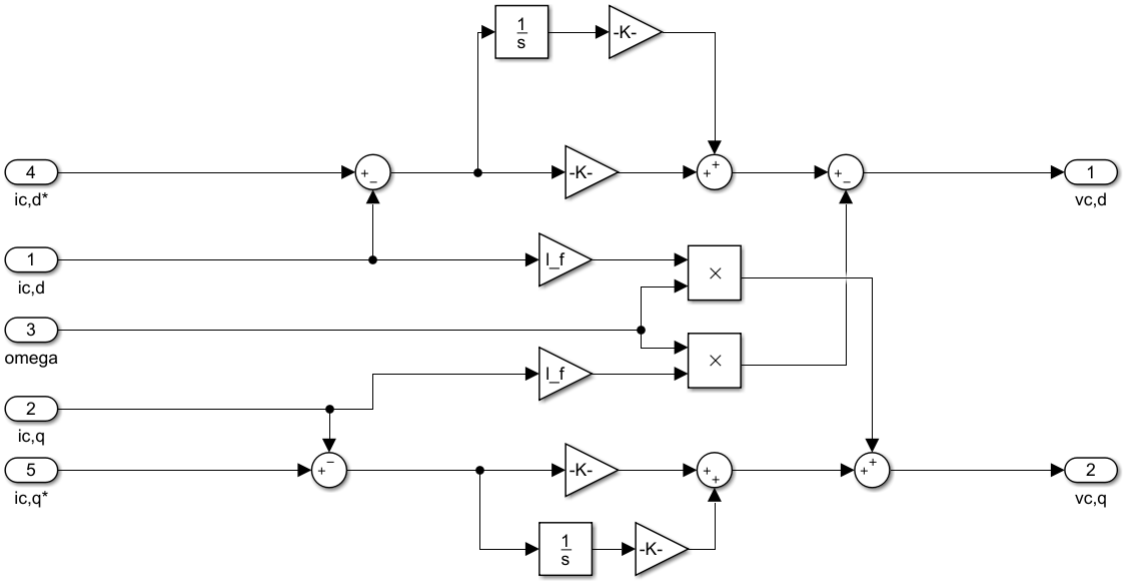

Figure 20: Current controller

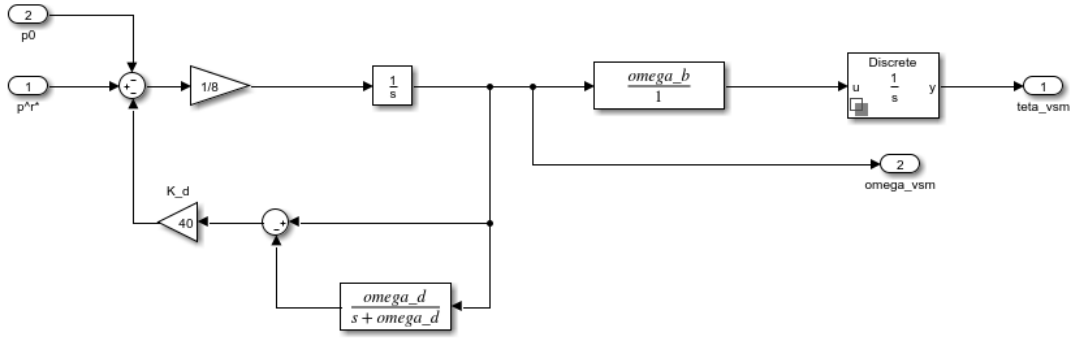

Figure 21: Inertia model.

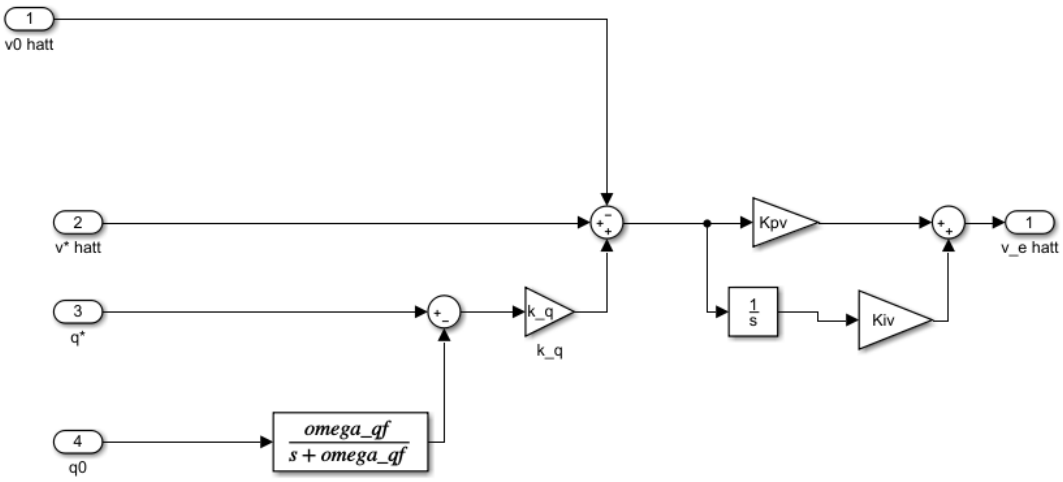

Figure 22: AVR.

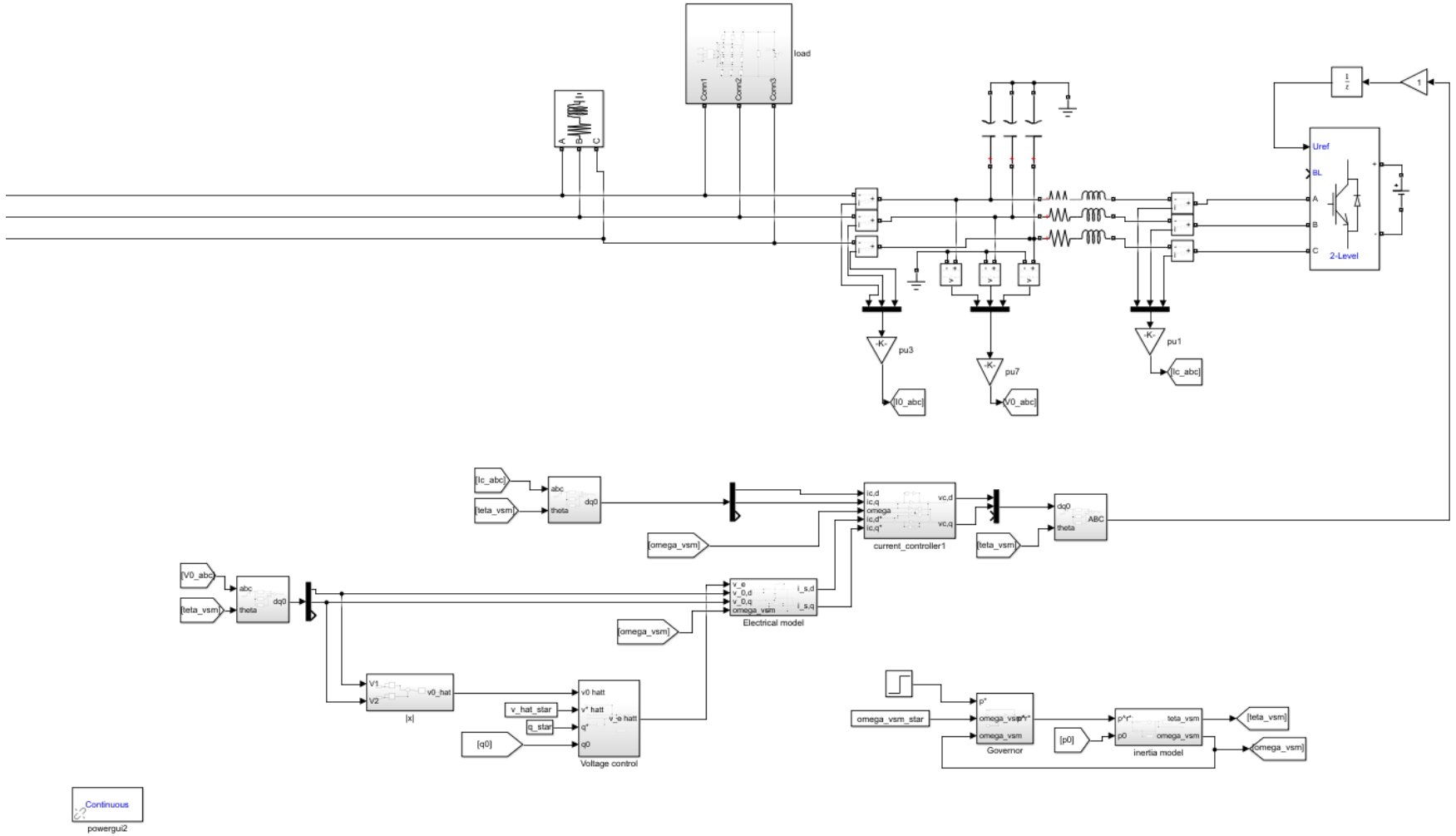

Figure 23: System model

8 Matlab Code

```
S_b_inverter = 884385*(1+0.833);
S_b_SM = 884385;
V_b = 690/sqrt(3/2);
I_b= S_b_inverter/(V_b*sqrt(3/2));
Z_b = V_b/I_b;
omega_b = 2*pi*50;
L_b = Z_b/omega_b;
C_b = 1/(Z_b*omega_b);

l_f = 0.08;
L_f = l_f*L_b;
r_f = 0.003;
R_f = r_f*Z_b;
c_f = 0.0074;
C_f = c_f*C_b;

r_g = 0.005;
R_g = r_g*Z_b;
l_g = 0.2;
L_g = l_g*L_b;

R_load = 0.5;
L_load = 0;

%% reference values
p_star = 0.5;
q_star = 0.0;
v_hat_star = 1.0;
omega_vsm_star = 1.0;

%% init current controller
T1_cc = L_f/R_f;%0.03;
Ti_cc = T1_cc;
Tsum_cc = 0.001;
Kp_cc = r_f*T1_cc/(2*Tsum_cc);
Ki_cc = 1/Ti_cc;%15;

%% Init inertia model
omega_g = 1.0; %pu
omega_d = 5; %rad/s
T_a = 3.5; %s
k_d = 40;

%% konvertering av pu sys
S_b_temp = 2750000;
V_b_temp = 690;
I_b_temp =  S_b_temp/(V_b_temp*sqrt(3/2));
Z_b_temp = V_b_temp/I_b_temp;
L_b_temp = Z_b_temp/omega_b;

```

```
51
52
53 R_s = Z_b_temp*0.1;
54 L_s = L_b_temp*0.25;
55 r_s = 0.1;
56 r_s2 = 0.001;
57 l_s = 0.25;
58
59 %% init voltage control
60 k_ffe = 0;
61 k_q = 0.1;%pu
62 k_pv = Kp_cc;
63 k_iv = Ki_cc*10;
64 omega_qf = 200;
65
66 %% Init Governor
67 k_omega = 20;
68
69 %% Init active damping
70 omega_ad = 50;
```